RADIO SCIENCE, VOL. 45, RS4006, doi:10.1029/2009RS004344, 2010

Improved estimates for neutral air temperatures at 90 km and 78°N using satellite and meteor radar data

M. E. Dyrland,[1] C. M. Hall,[2] F. J. Mulligan,[3] M. Tsutsumi,[4] and F. Sigernes[1]

Received 23 December 2009; revised 17 March 2010; accepted 31 March 2010; published 13 July 2010.

[1] A technique for using satellite-derived temperatures to calibrate initial estimates of 90 km temperatures measured by meteor wind radar is presented. Temperatures derived from the Nippon/Norway Svalbard Meteor Radar, situated on Svalbard at 78°N, 16°E, are calibrated using data from the Aura spacecraft's Microwave Limb Sounder (MLS) experiment. The calibration was performed in a two-step process: after an initial calibration of first-guess temperatures, results were used to adjust the MLS values to reflect daily means rather than the 0200–1100 UT observation period of the satellite instrument; thereafter the calibration was repeated with the revised MLS temperatures. The resulting temperature time series represents a marked improvement on earlier results calibrated using hydroxyl emission and potassium/K-Lidar observations, as the uncertainty is reduced from 17 to 7 K. These latest results represent a new step toward reliable and continual monitoring of upper mesosphere/lower thermosphere temperature.

Citation: Dyrland, M. E., C. M. Hall, F. J. Mulligan, M. Tsutsumi, and F. Sigernes (2010), Improved estimates for neutral air temperatures at 90 km and 78°N using satellite and meteor radar data, *Radio Sci.*, *45*, RS4006, doi:10.1029/2009RS004344.

1. Introduction

[2] Making measurements of absolute neutral air temperatures from the mesopause region (~80–100 km) has long been considered an important [*Jarvis*, 2001], but notoriously difficult task. The region is too high to reach for balloons and too low for in situ satellite measurements. Radars depend on gradients and discontinuities in refractive indices which are not always present in this part of the atmosphere. Optical measurements suffer from variable transmission and cloud conditions, and rockets are too expensive to keep continuous measurements with high temporal resolution running. Mesopause region temperatures are highly valuable input to atmospheric chemistry models, as well as potential tracers of atmospheric dynamics and global change [*Beig et al.*, 2003]. One of the problems is that most temperature retrieval algorithms are based on certain assumptions about the composition, the pressure or temperature gradients, the validity of thermodynamical equilibrium conditions, or other parameters [*Polaravapu et al.*, 2005]. This creates an ambiguity when interpreting the data as absolute neutral air temperatures. Measuring the temperature at high-Arctic latitudes (>75°N) is even more difficult, as there are few facilities and instruments available at these locations often because of logistical challenges due to a harsh climate. Furthermore, the temporal resolution and latitudinal coverage of satellite instruments are limited by their orbital mode and yaw maneuvers. Satellites in low Earth orbits with relatively low inclinations can only sporadically view high Arctic latitudes (e.g., the Upper Atmosphere Research Satellite (UARS) [*Reber et al.*, 1993]).

[3] One of the few high-Arctic locations where ground-based measurements have been performed over several decades is Adventdalen (78°N, 16°E), a valley close to the city Longyearbyen on the Svalbard archipelago. A long-term winter temperature series has been derived from spectral measurements of hydroxyl (OH) airglow emissions for the last three decades [*Sigernes et al.*, 2003]. However, these temperatures can only be retrieved for polar night conditions (November through February) and when there are relatively clear skies and low auroral activity [e.g., *Viereck and Deehr*, 1989].

[1]Department of Arctic Geophysics, University Centre in Svalbard, Longyearbyen, Norway.
[2]Tromsø Geophysical Observatory, University of Tromsø, Tromsø, Norway.
[3]Department of Experimental Physics, National University of Ireland, Maynooth, Ireland.
[4]National Institute of Polar Research, Tokyo, Japan.

0048-6604/10/2009RS004344

Meteor wind radars (MWRs) offer considerable potential for monitoring atmospheric temperatures near 90 km altitude. Unlike many optically based instruments, they are not limited by clouds or by the need for darkness, which allows them to operate unattended all year-round and for 24 h d^{-1}. Temperatures at 90 km can be deduced from the diffusion of meteor trails, and an approach, based on methods described by *Holdsworth et al.* [2006], was adopted by *Hall et al.* [2004] for obtaining temperatures from a meteor radar, specifically, in this case, also located in Adventdalen. Such measurements have the advantage that they can be made throughout the full day and for all seasons. The approach of *Hall et al.* [2004] involves calibration by an independent temperature series. Calibration by OH rotational temperatures (winter) and K-Lidar measurements (summer 2001–2003) have proven to yield overall realistic relative variations of the temperature at 90 km and the resulting time series for 2001–2006 was presented by *Hall et al.* [2006]. The calibration procedure was based on the assumption that the rotational temperature of the OH(6–2) band is representative of the neutral temperature at ~87 km altitude, an assumption that has been widely accepted and used [cf. *Sivjee*, 1992; *Beig et al.*, 2003]. The measured OH rotational temperatures were adjusted from 87 km to 90 km according to the temperature gradient from a model, before being used as calibration input for the temperatures measured by the meteor radar [*Hall et al.*, 2006].

[4] Recent studies have shown that the OH emission peak altitude can vary by several kilometers and that variations are particularly large at high-Arctic latitudes [*Winick et al.*, 2009]. Using satellite data they show that for extended periods during the winters 2004 and 2006, the OH emission peak was located well below 80 km and large zonal asymmetries were present within the Arctic region. Simultaneous ground-based and satellite measurements of OH airglow above Svalbard have revealed that the altitude variations are responsible for a large part of the fluctuations in the observed OH rotational temperatures [*Dyrland et al.*, 2010]. For periods of low OH emission peak altitude, the calibrated temperatures from the meteor radar might therefore be overestimated. The opposite is also possible, but more unlikely. Another recent study by *Mulligan et al.* [2009] presents an empirical formula for attributing a peak height to an OH rotational temperature measurement based on the observed intensity of the OH emissions. Still, we are left with the problem of limited data coverage, both seasonally and daily. There are, moreover, studies that indicate that the OH rotational temperatures from the 6–2 band are not necessarily representative of the neutral air temperatures [*Cosby and Slanger*, 2007]. Awareness of these issues has prompted us to look for other independent temperature measurements to act as input to the meteor radar temperature retrieval algorithm.

[5] Relatively recent launches of satellites probing the mesopause region have provided data sets that can be used for comparison with ground-based measurements. Some of these satellites have orbits with a high inclination angle to the equator which enables their onboard instruments to make observations at latitudes as high as ±80 degrees. The two instruments that are of particular interest for this study are SABER (Sounding of the Atmosphere by Broadband Emission Radiometry) on board TIMED (Thermosphere Ionosphere Mesosphere Energetics and Dynamics) which was launched in 2001, and MLS (Microwave Limb Sounder) on board the EOS (Earth Observing System) Aura spacecraft launched in 2004. In this study we again calibrate the Nippon/Norway Svalbard Meteor Radar (NSMR), situated on Svalbard at 78°N, 16°E, using Aura results (we will discuss why) and compare with determination from ground-based measurements of both OH(6–2) band radiance and K-Lidar backscatter, and also model predictions.

2. Instruments

[6] The NSMR (Nippon/Norway Svalbard Meteor Radar) radar is of the type meteor wind radar (MWR), often simply called a meteor radar [*Hocking et al.*, 2001]. The NSMR radar and the temperature retrieval technique are extensively described and discussed by *Hall et al.* [2004, 2006], and references therein and we only give a short resume here. The Svalbard system operates at 31 MHz with an altitude resolution of 1 km and effective time resolution of 30 min. Echoes from meteor trails are detected using an antenna array arranged as an interferometer; again, full details of the technique can be found via *Holdsworth et al.* [2006]. From these echoes, ambipolar diffusion coefficients D can be derived by measuring the radar echoes' decay time τ [*Chilson et al.*, 1996]. The two are related in the following way:

$$\tau = \frac{\lambda^2}{16\pi^2 D} \tag{1}$$

where λ is the radar wavelength. Using atmospheric pressure as input, temperatures can then be derived from the daily averaged ambipolar diffusion coefficients using the expression:

$$T = \sqrt{\frac{p \cdot D}{6.39 \cdot 10^{-2} K_0}} \tag{2}$$

where p (Pa) is the pressure and K_0 is the zero field mobility, which depends on the ion species in the meteor trail. K_0 is chosen according to *Cervera and Reid* [2000] and is assumed to be 2×10^{-4} m^2 s^{-1} V^{-1}. Pressure values

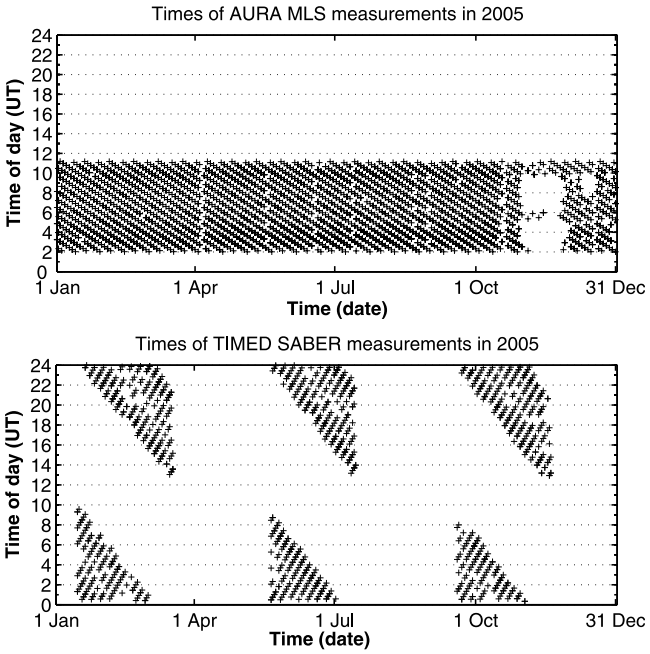

Figure 1. Typical temporal coverage of the Aura MLS and SABER instrument, in this case for 2005.

are derived from a combination of the empirical models of *Lübken and von Zahn* [1991] and *Lübken* [1999]. Ab initio, these values are appropriate for 70°N, 20°E, so *Hall et al.* [2006] adjusted them to 78°N by the meridional temperature gradient given by the NRLMSISE-00 model [*Picone et al.*, 2002]. A meteor radar at such a high latitude as 78°N suffers less from diurnal variation of meteor occurrence than at lower latitudes. This is because the majority of meteoroids lie in the plane of the ecliptic which is either completely above the horizon (summer) or not that far below it (winter) in polar regions [*Eshleman and Mlodnosky*, 1957]. Thus, calculating daily mean temperatures are believed to yield relatively small diurnal biases. In this paper we will refer to temperatures measured by the NSMR radar as NSMR temperatures.

[7] As mentioned earlier, to calibrate the radar data, measurements from two satellites can be considered: SABER on the TIMED satellite launched in 2001, and the MLS on the EOS Aura spacecraft launched in 2004. SABER scans the horizon and obtains temperatures from measurements of CO_2 15 μm limb emissions. The observed limb emission profiles are analyzed to produce vertical temperature profiles with approximately 2 km vertical resolution [*Mertens et al.*, 2004; *Remsberg et al.*, 2008]. The view of SABER is 90° to the right of the velocity vector of the TIMED spacecraft. Every 60–63 days the spacecraft switches between northward and southward looking yaw modes and it is only in the northward looking yaw mode that latitudes between 52°–83°N can be observed. Aura MLS looks forward from the spacecraft and samples continuously at all latitudes 82°S–82°N. *Schwartz et al.* [2008] found a 5–10 K bias between Aura MLS and SABER temperatures at 0.001 hPa (~96 km), the latter being higher, and comparisons made in connection with this study (not elaborated on here) indicate that this bias is larger in summer than winter for the northern hemisphere. Decisive in our choice of instrument for the subsequent calibration process is the temporal coverage of each satellite and we show these in Figure 1. The SABER times change according to the orbit of TIMED. This means that the daily averages are from different times of day in the course of a year and furthermore SABER data has three 60 day gaps in each year corresponding to a southward viewing yaw phase. In contrast, Aura MLS data are available on almost every day of the year from 0200 to 1100 UT. This fact and the reports of total errors in the order of ~10 K for the SABER summer temperatures due to noise and difficulties in the non-local-thermodynamical temperature retrieval algorithm [*Remsberg et al.*, 2008], made us select Aura MLS data as the optimal input for the NSMR calibration and we used Version 2.2 of the temperature retrieval algorithm [*Livesey et al.*, 2006].

[8] Satellite observations that occurred within the same days as NSMR measurements were identified. The spatial

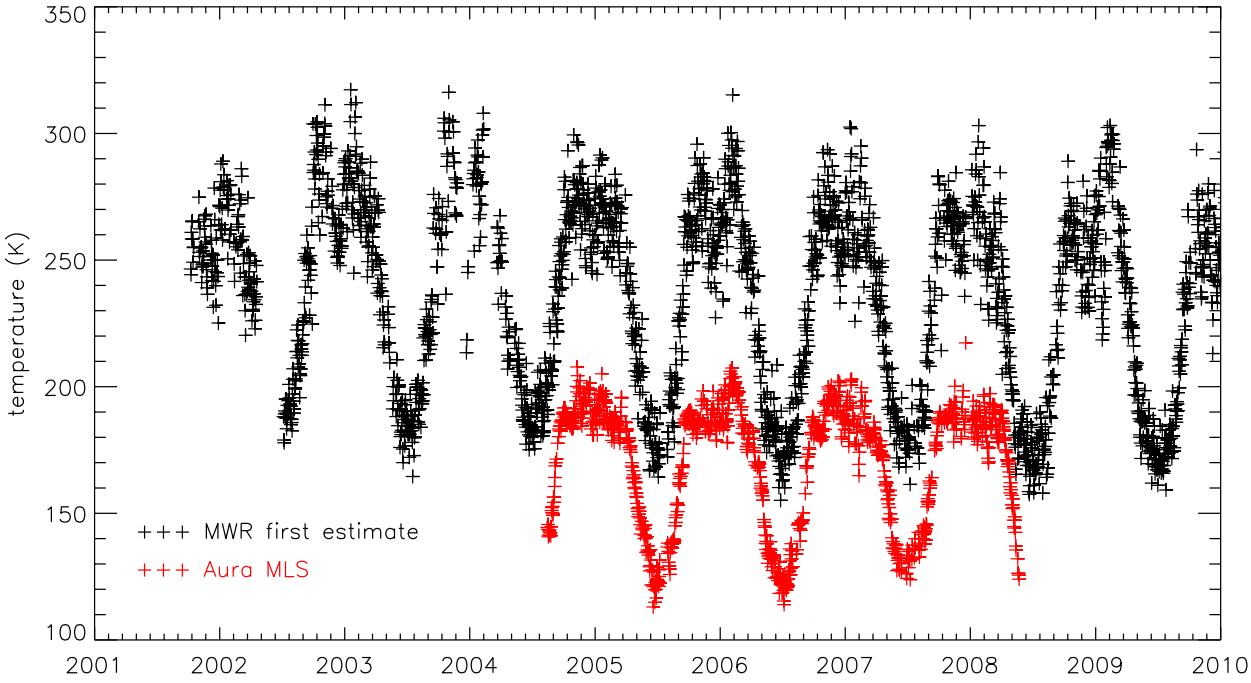

Figure 2. Raw temperatures from the NSMR derived using the method described in the text. Also shown are corresponding Aura MLS values to be used in the calibration.

criteria used to select Aura MLS measurements were 78 ± 5° N, 16 ± 10° E corresponding to a circle of approximately 600 km from the NSMR site. The data-quality screens specified by *Schwartz et al.* [2008] were applied to all of the Aura MLS data used. MLS temperature precision is quoted as approximately 3 K at 90 km, while vertical resolution is stated to be ~13 km at this altitude. The temperature values used as the starting point for the calibration of the NSMR data (corresponding to 90 km altitude) were obtained by linear interpolation from the values at the two altitudes that span this altitude.

3. Method and Results

[9] Using the method described in section 2, we determine daily mean temperatures from the echo fading times measured by NSMR and subsequent ambipolar diffusion coefficients for all available days since 1 October 2001, these being then regarded as a "first estimate" or "raw." Between 14 August 2004 and 22 April 2008 there were 1097 days when Aura MLS measurements coincided with NSMR measurements; both NSMR raw temperatures and Aura temperatures are shown in Figure 2 whence we can easily identify the clear systematic offset. A scatterplot of Aura determinations versus coincident NSMR ones is shown in Figure 3 together with a linear regression yielding the relation

$$T_{NSMR} = 1.44 T_{AuraMLS} - 9 \quad (3)$$

where T_{NSMR} and $T_{AuraMLS}$ are the NSMR and Aura MLS determined temperatures respectively, all values in Kelvin. In addition we separate out winter (November, December and January) and summer (May, June and July) days (shown by blue and orange in Figure 2) to illustrate qualitatively how the discrepancy between methods is seasonally dependent. As seen in equation (3), the slope of the linear fit was found to be 1.44 ± 0.02 KK^{-1} and the intercept found to be −9 ± 3 K and the next step is to apply these coefficients to the original NSMR data thus normalizing them to the Aura values. These results are not shown here because, as we shall see forthwith, they are only an intermediate step in the calibration process.

[10] So far we know little of the accuracy of the new NSMR temperatures; however, it is reasonable to assume that periodicities are real and that phases associated with them can be determined. Next, therefore, taking full advantage of the temporal resolution of the radar, 30 min, we examine the intraday variability of temperature relative to the corresponding mean for the day. These are then assembled into monthly average daily variations to

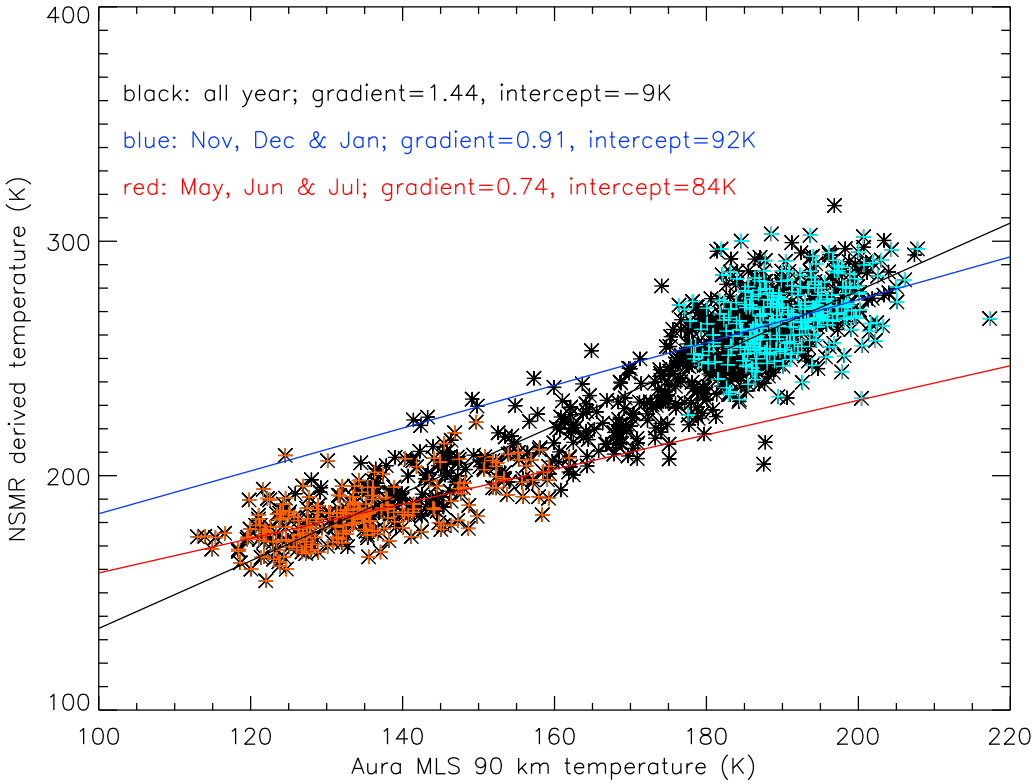

Figure 3. Scatterplot of NSMR derived temperatures versus those from Aura MLS together with the least absolute deviation linear fit. The black points show the entire data set (all months), and the black line the shows the corresponding linear fit. Superimposed on these are winter and summer month temperatures together with their corresponding linear fits and shown in blue and red, respectively.

yield the total tidal perturbation phase and amplitude (the latter to within the constraints imposed by the accuracy of equation (3)). Recalling now Figure 1, we see that the Aura measurements are not daily means as are the NSMR values, but are representative of the period 0200–1100 UT only and therefore the daily mean plus the tidal perturbation corresponding to the measurement period). Figure 4 shows monthly tidal perturbations as a function of time of day (applying the correction from equation (3) to the NSMR data in Figure 2) and we have also indicated 0200–1100 UT where Aura measured. The differences between monthly averages of the 0200–1100 UT (i.e., Aura measurement period) and 0000–2400 UT (i.e., NSMR measurement period) temperatures are given in Figure 5. Next we correct the Aura values by subtracting these measurement-period induced biases in order to arrive at daily mean temperatures that are indeed representative of the entire day, and perform a revised linear regression, akin to Figure 3. We wish to stress that in the absence of measurements of temperature at latitudes around 80°N, semiempirical models of the temperature tides are sparse. We therefore resort to a purely empirical approach consisting of determining biases solely due to sampling differences; although we intuitively know these are related to tides, we do not include any a priori assumptions as to tidal modes and their phases. The intercept now becomes zero (±2.7K) and the gradient reduces to 1.40 ± 0.02 KK^{-1} with a mean absolute deviation of 7 K. Calibrating the NSMR raw data now a second time, using the coefficients from this new iteration, yields the time series shown in Figure 6 where we have again included the Aura MLS values, this time after applying the seasonally varying correction indicated by Figure 5. In Figure 7 we now show a scatterplot of coincident NSMR and Aura values to give some appreciation of uncertainties. Although difficult to see, the points fall nearer the regression line following the adjustment for Aura observation time. The linear regression is indistinguishable from the line of zero intercept and gradient unity and we show the mean absolute deviations on either side of this. Superimposed are the K-Lidar temperatures where available [*Höffner and Lübken*, 2007]. Corresponding

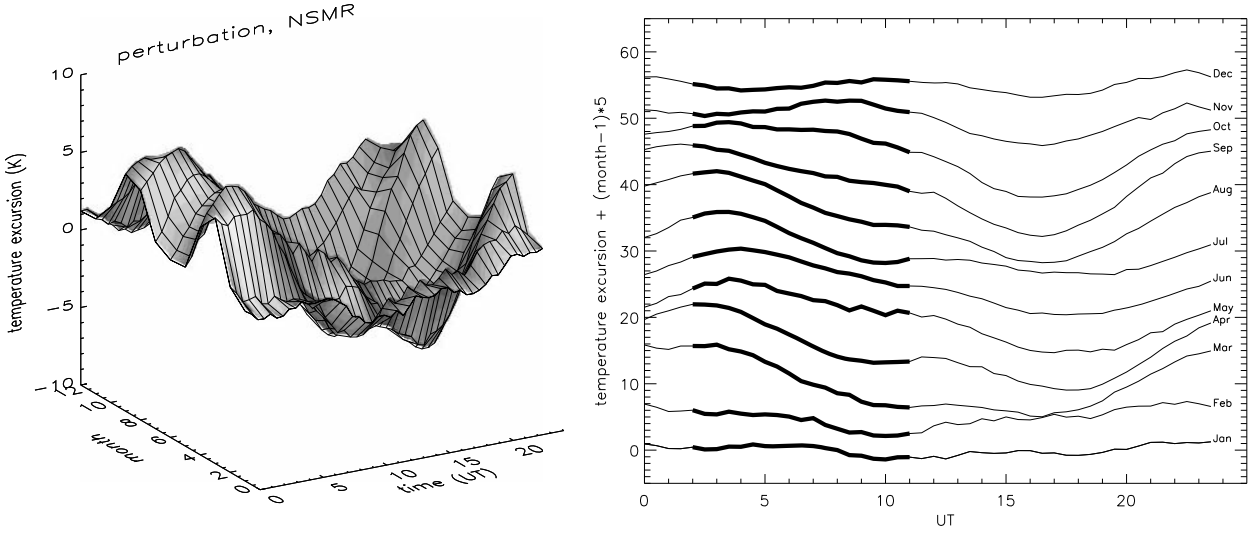

Figure 4. Monthly averages of intraday temperature excursions from the respective daily means as two portrayals. The time of day corresponding to Aura MLS observations, 0200–1100 UT, is highlighted (in which, for clarity, time series are displaced by 5 K per month subsequent to January).

rotational OH(6–2) [e.g., *Sigernes et al.*, 2003; *Hall et al.*, 2006] measurements, necessarily from winter days only explaining their grouping in the top right-hand part of the distribution, show systematically higher values however. As stated earlier, *Hall et al.* [2006] had presupposed the OH layer to be at a fixed height of 87 km and adjusted the temperatures to be representative of 90 km using gradients given by *Picone et al.* [2002]. *Mulligan et al.* [2009] and *Dyrland et al.* [2010] show this not to be the case, however, and that furthermore the height for which the OH-derived temperatures is representative is determined, at least in part, by the meridional wind. Other studies of OH temperatures and heights [e.g., *Azeem et al.*, 2007; *Viereck and Deehr*, 1989] confirm that calibration of NSMR by

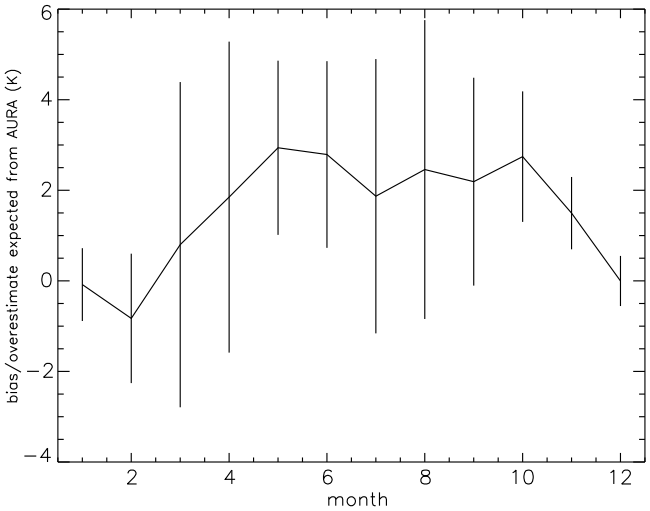

Figure 5. Bias incurred by Aura MLS only measuring in the period 0200–1100 UT as opposed to the full 24 h, as a function of season.

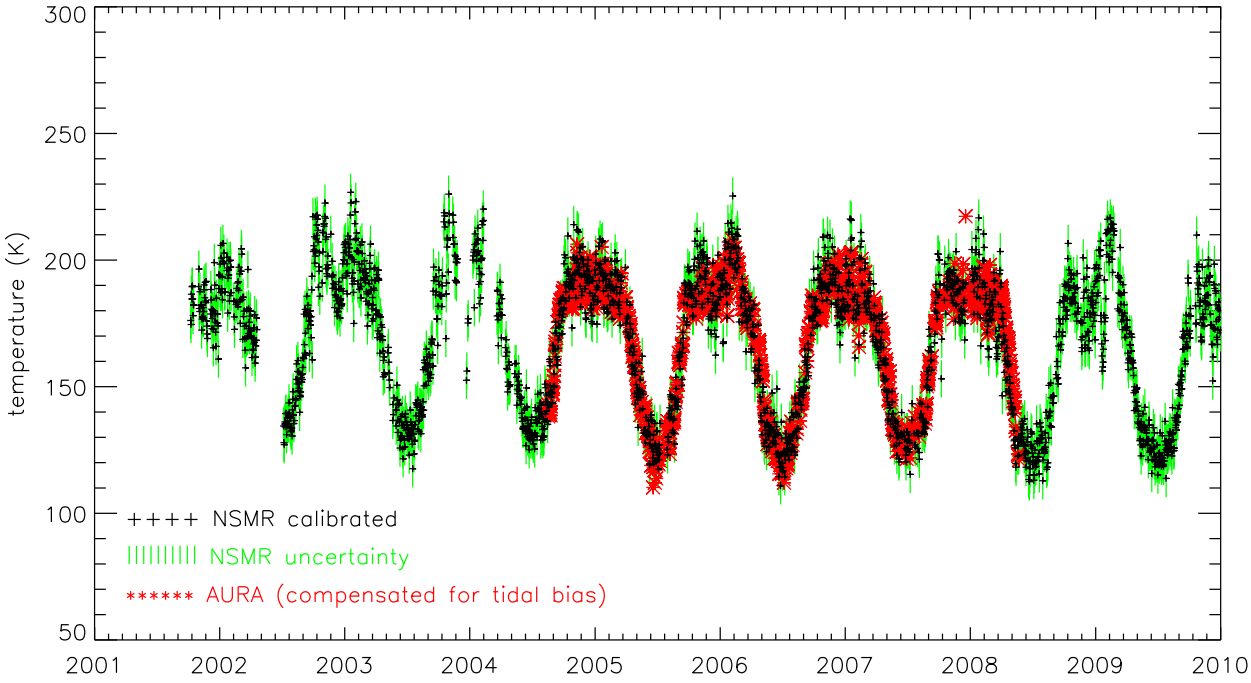

Figure 6. Final calibrated temperatures from NSMR (pluses) and with Aura MLS also shown (asterisks) after adjustment for observation period.

OH is not a simple task and that our strategy here, viz. using Aura MLS is an improvement on *Hall et al.* [2006].

4. Discussion

[11] Although NSMR detects enough echoes for 30 min averages to be computed, ambiguities may be introduced by the choice of input pressure for the analysis. As explained in section 2, daily values from *Lübken and von Zahn* [1991] and *Lübken* [1999], interpolated to higher latitudes using MSIS-00 [*Picone et al.*, 2002], are used as pressure input for the initial guess. These include seasonal variations, but not solar cycle or intraday variations. In the ideal world, climatological density or pressure data would be available for our latitude for us to test if the assumptions we make are valid, but unfortunately they are not.

[12] The inclusion of CIRA-86 model [*Rees et al.*, 1990] values in Figure 7 demonstrates how this model underestimates midrange (and therefore ~equinox temperatures), overestimates winter maximum and underestimates the depth of the summer minimum (i.e., overestimates the values themselves); similarly we see in Figure 7 how MSIS-00 [*Picone et al.*, 2002] systematically overestimates our values by 10–20 K and therefore we can concur with the findings of *Höffner and Lübken* [2007]. The discrepancy between NSMR and the MSIS-00 model is also in reasonable agreement with the findings of *Azeem et al.* [2007] (7.5 K) for Antarctic winter. That the K-Lidar temperatures shown in Figure 7 agree much better than the models and OH temperatures is reasonable, since they were performed by a colocated instrument with accurate height determination. Even so, we do not expect a perfect match since the atmospheric scattering volume is considerably smaller for the Lidar than that of NSMR.

[13] The greater spread in points in the top right-hand region of Figure 7 reflects the increased wave activity during the winter half of the year also seen clearly in the time series themselves as the modulation of the peaks in Figure 6. In such cases we could well anticipate differences between the relatively local NSMR measurements and those of Aura, justifying our strategy of performing a generalized linear regression between the two data sets and not attempting to construct a calibration that has a seasonal dependence.

[14] We have already emphasized that full year observations of diurnal variability in upper atmospheric temperatures above latitudes as high as Svalbard (78°N) are very sparse and this justifies our empirical approach in determining the diurnal bias of the Aura MLS temperatures, rather than resorting to model output. Figure 4 shows excursions from the daily mean of up to 5 K and it is interesting to compare these to other data. *Myrabø* [1984] observed 5 K amplitudes in ~87 km OH winter

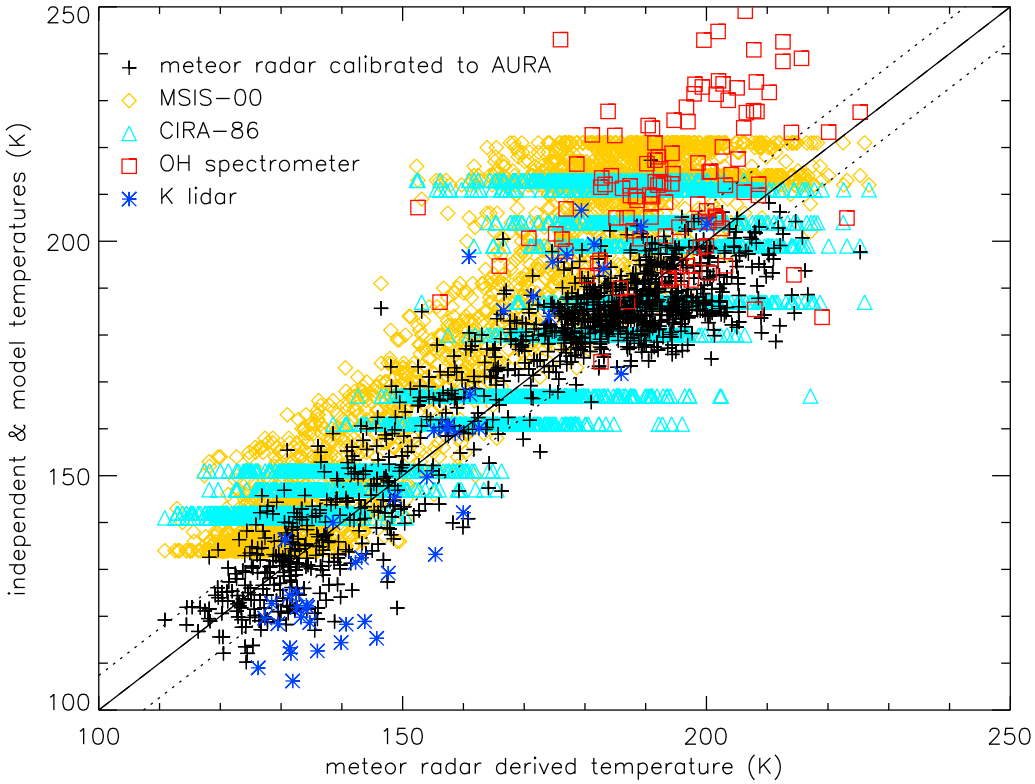

Figure 7. Scatterplot of coincident days of Aura MLS after adjustment for observation period versus NSMR temperature estimates following final calibration. Note that axes are reversed relative to Figure 3 because the NSMR temperatures now assume the role of independent variable. The regression line is indistinguishable from the zero-intercept unity gradient line, as should be expected. The dashed lines indicate the mean absolute standard deviation (7 K). Other coincident independent temperature determinations and model values are shown and discussed in the text.

temperatures from Svalbard which are in accordance with the NSMR measurements. *Höffner and Lübken* [2007] also investigated mean daily temperature fluctuations in their K-Lidar data from 2001 and found monthly averaged perturbations in the order of ~8 K and ~7 K at 90 km for March and July, respectively. This is a bit higher than what we find. However, the monthly averages were composed of only 11 and 16 daily averages and the criterion for creation of a daily average was that 3 h of measurements should be available. Furthermore, the Lidar was only operated in Svalbard from 2001 to 2003 and only for selected periods in the spring, summer and autumn of those years, so they are too sparse to form the basis for a climatology. However, the relatively good accordance between the K-Lidar and NSMR data both when it comes to the absolute value of the summer temperatures and the diurnal fluctuations, are reassuring.

[15] Ideally, we would also make a thorough comparison between the observed temperature perturbations and output from tidal models, e.g., the Global Scale Wave Model (GSWM) [*Hagan and Forbes*, 2002]. However, this model predicts very small (<1 K) diurnal and semidiurnal amplitudes at 78°N (according to values available for download at http://odo.colorado.edu/~zhangx/GSWM_extract.html). Studies have also shown that GSWM-model temperature amplitudes at 90 km and 69°N are considerably smaller than observations [e.g., *Singer et al.*, 2003]. According to our data and supported by *Höffner and Lübken* [2007], the discrepancy between model and observations at 78°N seem to be even larger.

5. Conclusions

[16] In this paper we have presented measurements of 90 km temperatures above the high Arctic location

Longyearbyen, Svalbard (78°N, 16°E). The temperatures were measured by ground-based meteor radar and then calibrated by MLS (Microwave Limb Sounder) on the Aura satellite. The calibration has been essentially a two-step process: after an initial calibration of first-guess temperatures, results were used to adjust the MLS values to reflect daily means rather than the 0200–1100 UT observation period; thereafter the calibration was repeated with the revised MLS temperatures. Earlier radar data had been calibrated using a combination of K-Lidar and OH rotational temperatures [*Hall et al.*, 2004, 2006] and the new approach has reduced the uncertainty to 7 K, compared to the previous value of 17 K. The K-Lidar measurements by *Höffner and Lübken* [2007] still agree well with our new results whereas the OH measurements do not, illustrating that earlier assumptions on the altitude of the OH layer may have been too simplistic. We also confirm the shortcomings of CIRA-86 and MSIS-00 at high latitude.

[17] As we have seen by the inclusion of NSMR diurnal temperature variation during the calibration steps, temperatures are, under normal operation, available every 30 min. While it cannot be understated that the meteor radar and other instruments complement each other, the radar method offers a temporal coverage not offered by either remote sensing or optical methods. By applying the above method to NSMR data from this and other locations with appropriate treatment of MLS values prior to final calibration, it will be possible to examine temperature variation, at least at 90 km, at all scales from tidal to climatic.

[18] **Acknowledgments.** The satellite data used in this study were acquired as part of the activities of the NASA Earth-Sun System Division, and are archived and distributed by the Goddard Earth Sciences (GES) Data and Information Services Center (DISC). We are highly appreciative of the NASA EOS Aura MLS and NASA TIMED SABER teams for providing free access to the data. We are also grateful to Chuck Deehr at the Geophysical Institute, University of Alaska Fairbanks, and Takehiko Aso, National Institute of Polar Research, Tokyo, for their initiatives for putting the ground-based instruments in Svalbard and for sharing the data. We would also like to thank the two anonymous reviewers for their valuable input.

References

Azeem, S. M. I., G. G. Sivjee, Y.-I. Won, and C. Mutiso (2007), Solar cycle signature and secular long-term trend in OH airglow temperature observations at South Pole, Antarctica, *J. Geophys. Res.*, *112*, A01305, doi:10.1029/2005JA011475.

Beig, G., et al. (2003), Review of mesospheric temperature trends, *Rev. Geophys.*, *41*(4), 1015, doi:10.1029/2002RG000121.

Cervera, M. A., and I. M. Reid (2000), Comparison of atmospheric parameters derived from meteor observations with CIRA, *Radio Sci.*, *35*, 833–843.

Chilson, P. B., P. Czechowsky, and G. Schmidt (1996), A comparison of ambipolar diffusion coefficients in meteor trains using VHF radar and UV lidar, *Geophys. Res. Lett.*, *23*, 2745–2748.

Cosby, P. C., and T. G. Slanger (2007), OH spectroscopy and chemistry investigated with astronomical sky spectra, *Can. J. Phys.*, *85*, 77–99, doi:10.1139/P06-088.

Dyrland, M. E., F. J. Mulligan, C. M. Hall, F. Sigernes, M. Tsutsumi, and C. S. Deehr (2010), Response of OH airglow temperatures to neutral air dynamics at 78°N, 16°E during the anomalous 2003–2004 winter, *J. Geophys. Res.*, *115*, D07103, doi:10.1029/2009JD012726.

Eshleman, V. R., and R. F. Mlodnosky (1957), Directional characteristics of meteor propagation derived from radar measurements, *Proc. IRE*, *45*(12), 1715–1723.

Hagan, M. E., and J. M. Forbes (2002), Migrating and nonmigrating diurnal tides in the middle and upper atmosphere excited by tropospheric latent heat release, *J. Geophys. Res.*, *107*(D24), 4754, doi:10.1029/2001JD001236.

Hall, C. M., T. Aso, M. Tsutsumi, J. Höffner, and F. Sigernes (2004), Multi-instrument derivation of 90 km temperatures over Svalbard (78°N 16°E), *Radio Sci.*, *39*, RS6001, doi:10.1029/2004RS003069.

Hall, C. M., T. Aso, M. Tsutsumi, J. Höffner, F. Sigernes, and D. A. Holdsworth (2006), Neutral air temperatures at 90 km and 70°N and 78°N, *J. Geophys. Res.*, *111*, D14105, doi:10.1029/2005JD006794.

Hocking, W. K., B. Fuller, and B. Vandepeer (2001), Real-time determination of meteor-related parameters utilizing modern digital technology, *J. Atmos. Sol. Terr. Phys.*, *63*, 155–169.

Höffner, J., and F.-J. Lübken (2007), Potassium lidar temperatures and densities in the mesopause region at Spitsbergen (78°N), *J. Geophys. Res.*, *112*, D20114, doi:10.1029/2007JD008612.

Holdsworth, D. A., R. J. Morris, D. J. Murphy, I. M. Reid, G. B. Burns, and W. J. R. French (2006), Antarctic mesospheric temperature estimation using the Davis MST radar, *J. Geophys. Res.*, *111*, D05108, doi:10.1029/2005JD006589.

Jarvis, M. J. (2001), Bridging the atmospheric divide, *Science*, *293*, 2218–2219, doi:10.1126/science.1064467.

Livesey, N. J., W. V. Snyder, W. G. Read, and P. A. Wagner (2006), Retrieval algorithms for the EOS Microwave Limb Sounder (MLS), *IEEE Trans. Geosci. Remote Sens.*, *44*, 1144–1155.

Lübken, F.-J. (1999), Thermal structure of the Arctic summer mesosphere, *J. Geophys. Res.*, *104*, 9135–9149.

Lübken, F.-J., and U. von Zahn (1991), Thermal structure of the mesopause region at polar latitudes, *J. Geophys. Res.*, *96*, 20,841–20,857.

Mertens, C. J., et al. (2004), SABER observations of mesospheric temperatures and comparisons with falling sphere measurements taken during the 2002 summer MacWAVE

campaign, *Geophys. Res. Lett.*, *31*, L03105, doi:10.1029/2003GL018605.

Mulligan, F. J., M. E. Dyrland, and F. Sigernes (2009), Inferring hydroxyl layer peak heights from ground-based measurements of OH(6–2) band integrated emission rate at Longyearbyen (78°N, 16°E), *Ann. Geophys.*, *27*, 4197–4205.

Myrabø, H. K. (1984), Temperature variation at mesopause level during winter solstice at 78°N, *Planet. Space Sci.*, *32*(2), 249–255.

Picone, J. M., A. E. Hedin, D. P. Drob, and A. C. Aikin (2002), NRLMSISE-00 empirical model of the atmosphere: Statistical comparisons and scientific issues, *J. Geophys. Res.*, *107*(A12), 1468, doi:10.1029/2002JA009430.

Polaravapu, S., T. G. Shepherd, Y. Rochon, and S. Ren (2005), Some challenges of middle atmosphere data assimilation, *Q. J. R. Meteorol. Soc.*, *131*, 3513–3527, doi:10.1256/qj.05.87.

Reber, C. A., C. E. Trevathan, R. J. McNeal, and M. R. Luther (1993), The Upper Atmosphere Research Satellite (UARS) mission, *J. Geophys. Res.*, *98*(D6), 10,643–10,647.

Rees, D., J. J. Barnett, and K. Labitzke (1990), CIRA 1986, Part II, Middle Atmosphere Models, *Adv. Space Res.*, *10*(12), 519 pp.

Remsberg, E. E., et al. (2008), Assessment of the quality of the Version 1.07 temperature-versus-pressure profiles of the middle atmosphere from TIMED/SABER, *J. Geophys. Res.*, *113*, D17101, doi:10.1029/2008JD010013.

Schwartz, M. J., et al. (2008), Validation of the Aura Microwave Limb Sounder temperature and geopotential height measurements, *J. Geophys. Res.*, *113*, D15S11, doi:10.1029/2007JD008783.

Sigernes, F., N. Shumilov, C. S. Deehr, K. P. Nielsen, T. Svenøe, and O. Havnes (2003), Hydroxyl rotational temperature record from the Auroral Station in Adventdalen, Svalbard (78°N, 15°E), *J. Geophys. Res.*, *108*(A9), 1342, doi:10.1029/2001JA009023.

Singer, W., J. Bremer, W. K. Hocking, J. Weiss, R. Latteck, and M. Zecha (2003), Temperature and wind tides around the summer mesopause at middle and Arctic latitudes, *Adv. Space Res.*, *31*(9), 2055–2060.

Sivjee, G. G. (1992), Airglow hydroxyl emissions, *Planet. Space Sci.*, *40*, 235–242.

Viereck, R. A., and C. S. Deehr (1989), On the interaction between gravity waves and the OH Meinel (6–2) and the O_2 atmospheric (0–1) bands in the polar night airglow, *J. Geophys. Res.*, *94*, 5397–5404.

Winick, J. R., P. P. Wintersteiner, R. H. Picard, D. Esplin, M. G. Mlynczak, J. M. Russell III, and L. L. Gordley (2009), OH layer characteristics during unusual boreal winters of 2004 and 2006, *J. Geophys. Res.*, *114*, A02303, doi:10.1029/2008JA013688.

M. E. Dyrland and F. Sigernes, Department of Arctic Geophysics, University Centre in Svalbard, PO Box 156, N-9171 Longyearbyen, Norway. (margit.dyrland@unis.no; fred.sigernes@unis.no)

C. M. Hall, Tromsø Geophysical Observatory, University of Tromsø, N-9037 Tromsø, Norway.

F. J. Mulligan, Department of Experimental Physics, National University of Ireland, Maynooth, Ireland.

M. Tsutsumi, National Institute of Polar Research, Tokyo 173-8515, Japan.